

## Paleoearthquake evidence in Tenerife (Canary Islands) and possible seismotectonic sources

L.I. Gonzalez de Vallejo<sup>1</sup>, R. Capote<sup>1</sup>, L. Cabrera<sup>2</sup>, J.M. Insua<sup>1</sup> and J. Acosta<sup>3</sup>

<sup>1</sup>Dpto. de Geodinámica, Universidad Complutense, 28040 Madrid, Spain. (vallejo@geo.ucm.es)

<sup>2</sup>Laboratorio COAC, 38509 Guimar, Tenerife, Spain

<sup>3</sup>Instituto Español de Oceanografía, C/ Corazón de María 8, 28002 Madrid, Spain

*Key words:* Canary Islands, Paleoliquefaction, Paleosismicity, Seismites, Seismotectonic, Tenerife

### Abstract

A series of clastic dikes and tubular vents were identified in southern Tenerife (Canary Islands). These features are the result of seismic liquefaction of a Holocene sand deposit, as the consequence of a high intensity paleoearthquake. The peak ground acceleration (pga) and magnitude of the paleoearthquake generating these liquefaction features were estimated by back calculation analysis. A representative value of  $0.30 \pm 0.05$  g was obtained for the pga. From this, an earthquake intensity of IX was estimated for the liquefaction site. Magnitude bound methods and energy based approaches were used to determine the magnitude of the paleoearthquake, providing a moment magnitude  $M = 6.8$ . The zone in which the liquefaction structures are found has undergone tectonic uplift and is affected by two faults. One of these faults was responsible for displacing Holocene materials. Dating of the uplifted sand formation indicates an age of  $10,081 \pm 933$  years, the liquefaction features ranging from this age to  $3490 \pm 473$  years BP. This paleoearthquake was of much greater magnitude than those known historically. Faults with neotectonic activity are significant features that should be borne in mind when assessing the seismic hazards of the Canary Islands, presently considered as low and mainly of volcanic origin.

### Introduction and regional seismicity

Several structures attributed to liquefaction phenomena of seismic origin have been identified in exposed sand deposits near El Médano, on the south coast of Tenerife, Canary Islands (Figure 1). These findings prompted subsequent tectonic investigations including the geotechnical characterization of soils, geochronological analysis, and the analysis of geophysical, seismicity, and neotectonic data which we report here. In these investigations, we were able to characterize a Holocene sand formation and analyze the liquefaction structures. Possible formation mechanisms and the origin and age of these structures were evaluated. In the same area, we identified two faults that affected the Holocene deposits. Estimates were made of the acceleration and magnitude of the paleoearthquake that produced these structures, and possible seismic sources were characterized

Based on earthquake information, the Canary Islands have been generally thought to experience low to very low seismicity, with earthquakes always associated with volcanic activity. During the historical period (Figure 2A), which starts in the XIV century with the first references to volcanic eruptions, the most intense earthquakes on the archipelago took place in Yaiza (Lanzarote) in 1730 (intensity X), in Fuencaliente and Cumbre Vieja (La Palma) in 1677 and 1920, respectively (both VII), in Ingenio (Gran Canaria) in 1913 (VII), and in Fuerteventura in 1915 and 1917 (both VII). On the island of Tenerife, the maximum intensity recorded was VI for the earthquakes on 1910/03/15 in Icod, 1909/01/4 in Puerto de la Cruz, 1909/09/23 in La Orotava, 1909/11/21 in Vilaflor and 1937/06/21 in Garachico. In this historic record, six earthquakes of intensity VI were registered on Tenerife, all in the 20th century and mostly affecting the north side of the island or its capital city Santa Cruz.

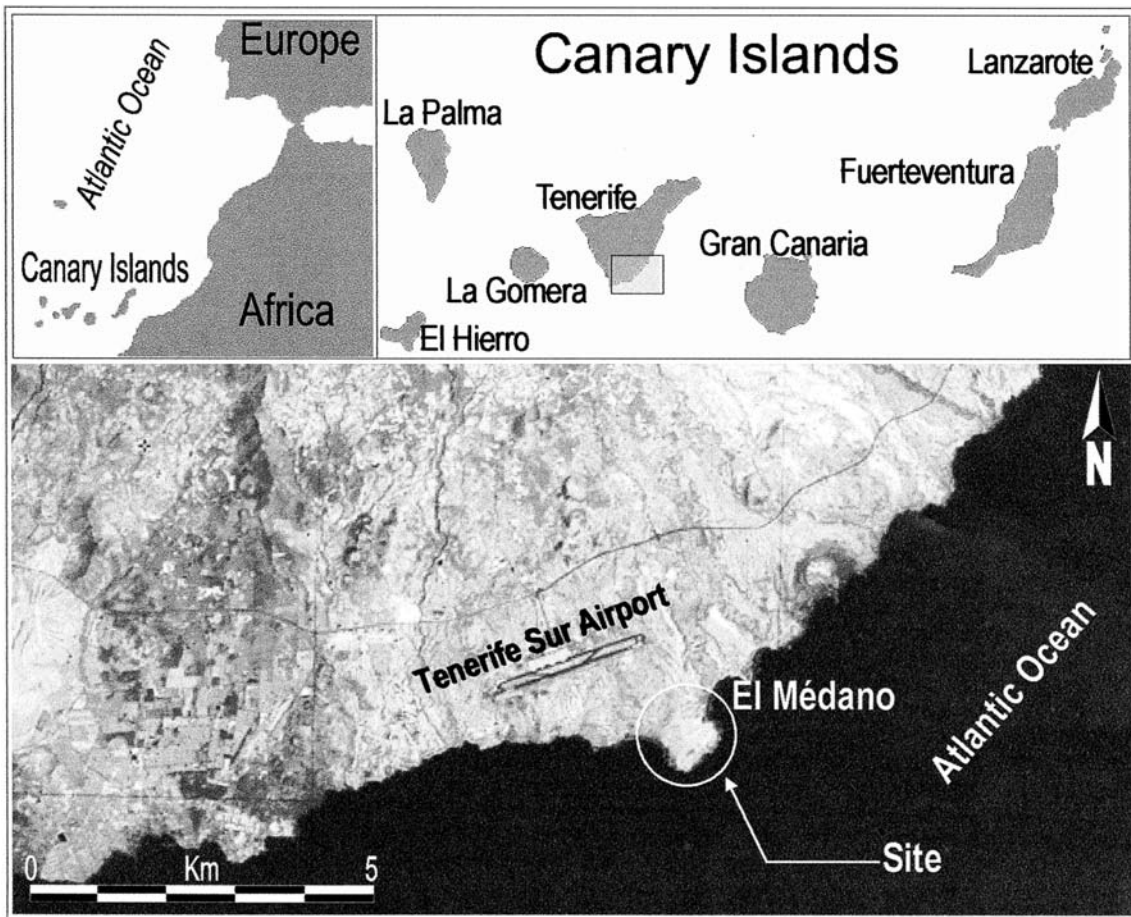


Figure 1. General location of the study area.

This record only reflects earthquakes felt in the most highly populated areas or those associated with volcanic eruptions. Knowledge of events occurring on the islands of El Hierro, La Gomera or the south of Tenerife is practically non-existent.

It was not until 1958 that a seismological station was installed in the Canaries. Two further stations were built in 1975, and over the past few years a more extensive network is being set up, with plans for stations over all the islands (there were seven stations in 2002). This will allow greater precision in locating and characterizing earthquakes. The distribution of epicenters recorded over the instrumented period is shown in Figure 2B.

The largest instrumented earthquake had a moment magnitude  $M = 5.2$ , its epicenter being in the sea between the islands of Tenerife and Gran Canaria ( $27^{\circ}56.8' N$  and  $16^{\circ}12.0' W$ ). Its maximum intensity was even felt on Tenerife. An analysis of this

earthquake (Mezcua et al., 1992) has provided some ideas regarding the seismotectonic setting of the Canaries, which could help explain the paleoearthquake that caused the paleoliquefaction discussed here. The distribution of aftershocks recorded by a temporary station set up on the south coast of Tenerife between May 9 and June 17, 1989 indicates concentrated aftershocks along an 80 km long band aligned  $N33^{\circ}$  (Figure 2C). This earthquake corresponds to a fault of around 30 km length. The hypocenter depth of the 5.2 magnitude event has been calculated as 50 km by Mezcua et al. (1992) and as 15 km by Dziewonski et al. (1990).

The analysis of the focal mechanism and that of the aftershocks points to a NNE-SSW alignment and inclination close to the vertical for the fault. This fault could also have been responsible for seismicity of greater magnitude and not related to processes of volcanic activity. Further more, geophysical marine

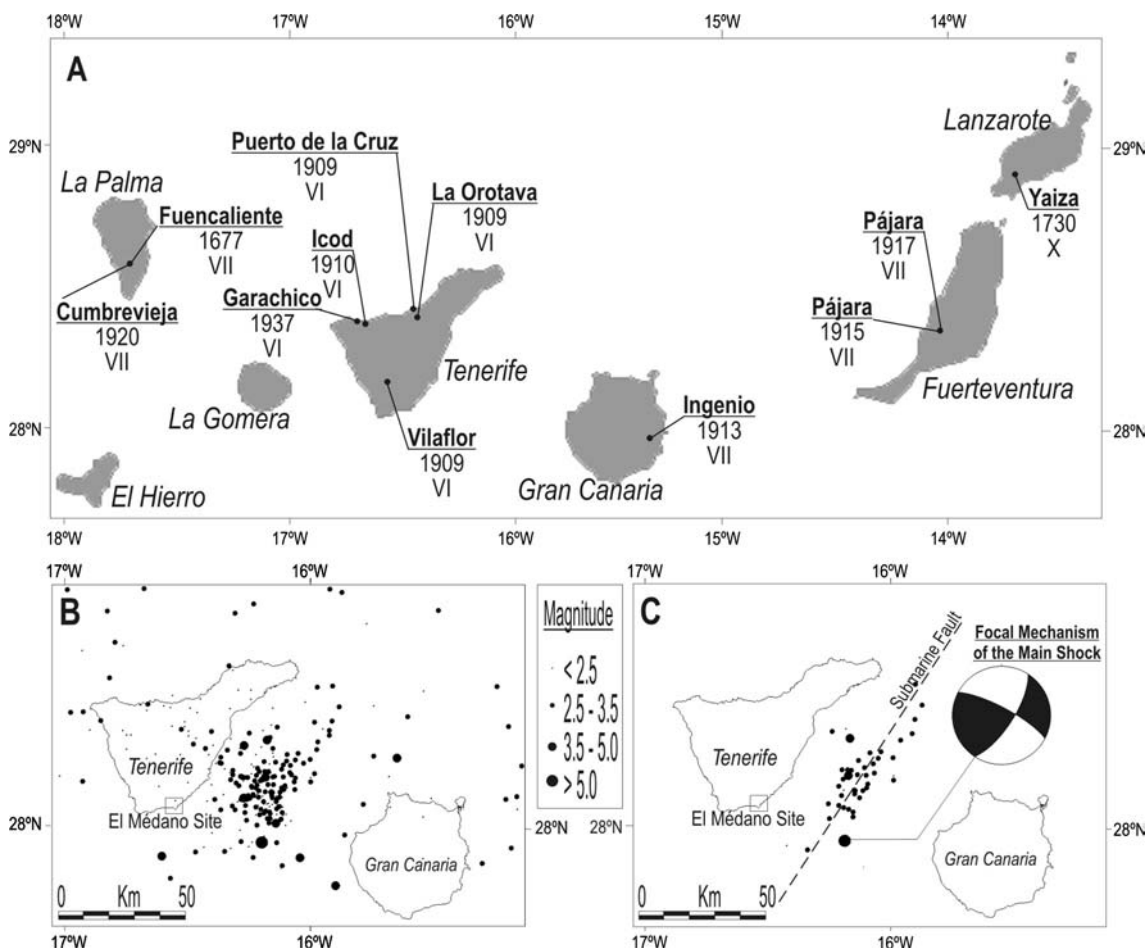


Figure 2. Seismicity of the Canary Islands. A: Historical seismicity until 1975 for earthquakes of intensity  $I \geq VI$ . B: Earthquake epicenters from 1975 to 2002 between Tenerife and Gran Canaria. C: Epicenters of the 1989 earthquake and its aftershocks. Nodal planes from focal mechanism: A =  $33^\circ-71^\circ$  SE; B =  $298^\circ-77^\circ$  NE.

investigations have revealed the occurrence of significant tectonic events (Llanes et al., this volume) associated with epicenters in the sea.

There is an obvious need for investigations that focus on paleoseismicity and neotectonics in regions for which earthquake information is scarce. This is definitely the case for the Canary Islands, whose instrumental period is shorter than 30 years and historical record is incomplete.

### Geology of the Study Area

The area investigated is found in El Médano close to Leocadio Machado Beach (Figure 3). This beach is bounded inshore by a 40–50 meter wide range of coastal dunes orientated in a NE–SW direction. Some

small lagoons have formed between the dunes and a coastal platform. This platform overlies a formation of volcanic tuffs of acid composition, and descends from the volcanic central part of the island. Towards the SW, a minor volcanic structure, the Montaña Roja, is composed of pyroclastic basaltic materials that overlie the tuff formation. These materials are overlain by a formation comprising beach sands that rises 2 to 15 m above sea level and shows several liquefaction structures.

The tuffs correspond to a set of pyroclastic units related to a phase of explosive salic eruptions between 0.7 and 0.13 Ma. The material is composed of pumice lapilli, lithic fragments and sanidine crystals. The Montaña Roja volcano lies at the southern margin of the study area (Figure 3). The volcano is a breached cone, open towards the ESE. Its altitude

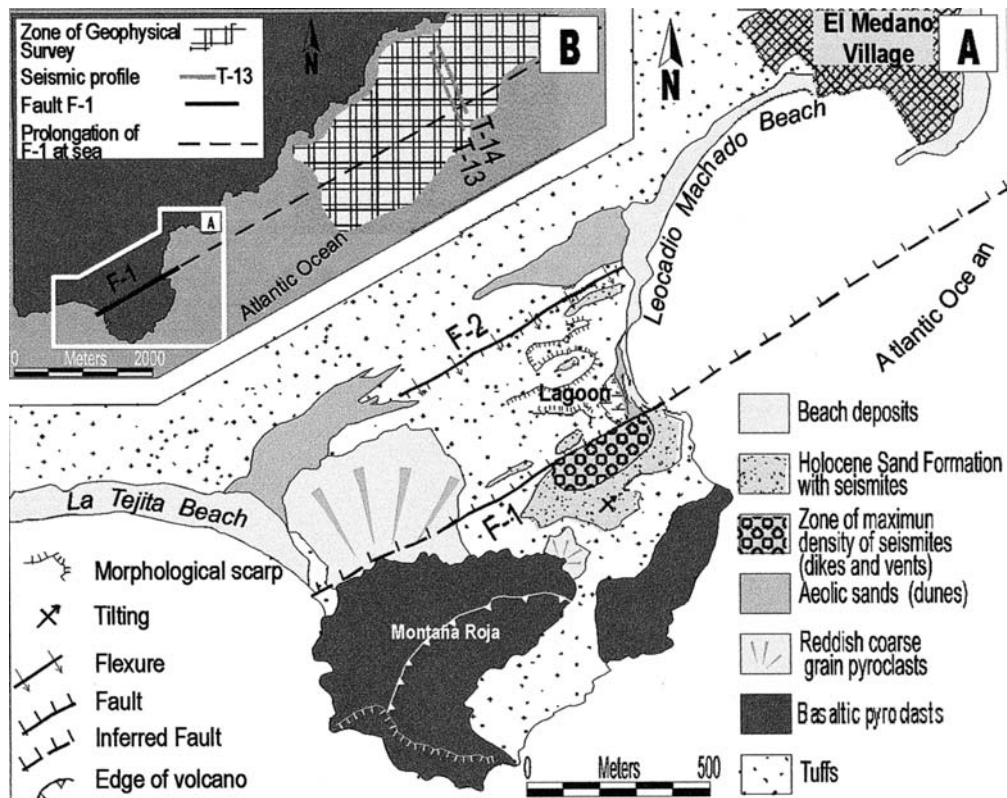


Figure 3. El Médano Site. A: Geological sketch map showing liquefaction features. B: Seismic profiles and prolongation of fault F-1 into the sea.

is 150 m above the lowlands at its base. It is composed of basaltic ash and cinder type pyroclasts and has been dated as being older than 100,000 years. The beach sand formation comprises bioclastic sands or weakly cemented, compact calcarenites and is 2.0 to 2.5 m thick. The coarse sand is made up of shell fragments, lithic grains, and plagioclase and pyroxene crystals. The substrate is composed of massive salic tuffs, within which an alteration level or softer paleosol 0.5 m thick can be observed. At some points, it is easy to distinguish a dense network of plant root structures, indicating the beach is transgressive and lies upon a densely vegetated surface. In turn, the beach material is covered in some areas by a thin pyroclastic level < 1 m thick and by calcareous crusts. The pyroclastic level contains centimetric-size, yellowish, pumice fragments enveloped by a pumice matrix. The white carbonate crust is laminated and 0.1 m thick.

The beach sand formation is slightly inclined at 3.5° towards the NE and is fractured such that faults and a network of joints organized in sets may be observed. The most outstanding tectonic structures are

two N55° E trending faults (F1 and F2) running from Leocadio Machado Beach towards the SW (Figure 3). The southern fault F1 is most evident and is marked by an escarpment of 0.7 to 1.2 m height, SE side up, interrupting the beach and chain of coastal dunes, and also bounding the inland lagoon. The scarp disappears towards the SW and the fault's course appears to be covered by recent dunes and a reddish-colored basaltic pyroclastic deposit coating the NW flank of Montaña Roja volcano. The trace of fault F1 can be followed 1.2 km onshore, although it extends under the sea at both its exposed ends. In fact, several seismic reflection profiles were performed in the surroundings of El Médano in the bay's offshore zone. The profiles were obtained using a UNIBOOM system (EG&G) on a catamaran with an 8-element hydrophone, firing 500J as the energy source. The ship was positioned using a Raydist system with two shore-stations working in circular mode. The profiles indicate an acoustic basement and a top series of unconsolidated Quaternary sediments. A NE-SW trending fault cutting the acoustic basement was detected along the trace of fault

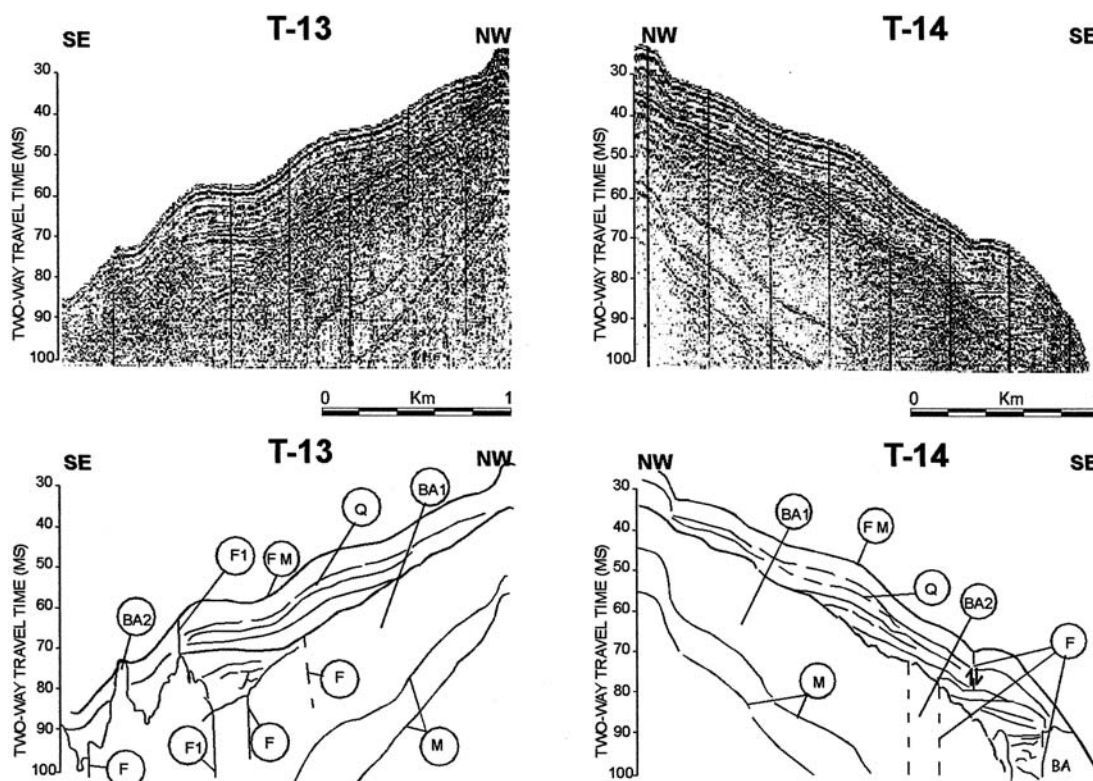


Figure 4. Seismic profiles. Upper panel: Seismic reflection Uniboom profile T-13 and T-14 off the El Médano coast (see Figure 3 for location). Lower panel: Interpretation drawing: FM: Sea floor. Q: Quaternary sediments; BA1: Acoustic basement type 2; F1: Fault F1; F: other fractures; M: Multiple.

F1 (Figure 4). The minimum length of this fault is 5 km.

The northern fault, F2 (Figure 3), is marked by a less pronounced morphological scarp. This fault is best observed at the NE extreme of the mapped area and fades out until it disappears at the SW end. The fault is marked by a slight flexure that produces a scarp 0.5 m high with more erosion of the footwall. A vertical displacement of 0.7 to 1.2 m has been observed in fault F1. The time of the displacements was after formation of the beach, dated as Holocene as described below.

A set of highly continuous fractures interpreted as joints mainly affects the tuff formation. Some of these joints, nevertheless, show an intensely curved trace. Although relatively small in number for the area, their inclinations were always close to 90° vertical. The most common alignments define three sets of joints whose directions in order of highest to lowest frequency are N175°, N56° and N105° (Figure 5).

#### Description of the liquefaction features

Liquefaction structures were observed in the uplifted beach sand formation (Figures 3 and 6). This formation extends over an area of around 90,000 m<sup>2</sup>, but could have reach 650,000 m<sup>2</sup> in the past 50 years. Changes produced in coastal dynamics and anthropogenic effects have substantially modified the zone over the last decades, with the almost complete disappearance of the dunes and acceleration of erosive processes. Artificial removal of a large proportion of the uplifted beach sands has led to the current appearance of the study area.

The section observed in the site was as follows from top to bottom:

- An upper layer H1 located at the top of the deposit composed of coarse to intermediate, highly compact, partially-cemented sands. Its thickness is approximately 1 m. The surface is intensely eroded and shows wind erosion structures indicating its

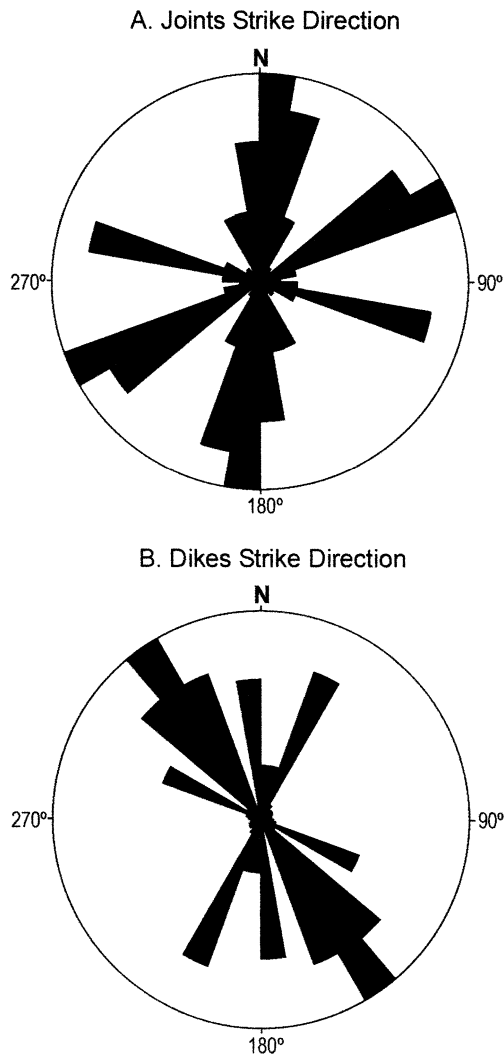


Figure 5. Rose diagrams displaying the two dimensional orientation distribution of data in the form of a circular histogram. A: Joint strike direction; B: Dike strike direction.

thickness was greater, possibly attaining at least 2 m. This layer shows evidence of liquefaction structures, sand dikes and vents described below. Above this layer, small calcareous crusts of 1–10 cm thickness and altered tuffs appear.

- The lower layer H2, beneath the previous layer, is comprised of medium to coarse sands, somewhat finer and less compact than in layer H1. It shows lamination and cross-stratification. This layer is partially crossed by vents but no dikes are observed. Its thickness ranges from 0.5 to 1 m.
- The substrate is composed of two layers of tuffs, T1 at the top and T2 at bottom. T1 comprises reddish tuffs weathered to form a 0.5 m thick

paleosol. T2 is formed by yellowish, massive, highly compact pumice tuffs.

Within layers H1 and H2 there are numerous liquefaction structures formed by vents and clastic dikes or tabular structures (Figures 7 and 8). These outcrop both at the surface or in natural exposures. The dikes are composed of sands of the same composition as in layer H2, with strikes of 145°, 25°, 5° and 110° (Figure 5). The 145° striking dikes, besides being the most frequent, lie almost perpendicular to the direction of the topographical slope, while those trending 110° show similar directions to the 105° striking joints. In the mapped area, the length of the dikes reaches 25–30 m, although they are not easy to observe because of the intense erosion and dune deposits that partly cover them. Dikes are commonly 4 to 8 cm thick, although in some cases, thicknesses of up to 20 cm have been measured. Many of these dikes have a central opening or double rim 0.5 to 1.0 cm wide (Figure 9). The main system (145°) is the most continuous and presents the greatest thicknesses. The dikes show lateral terminations in the shape of thin filaments up to 1 cm long. Sometimes they cut into each other and also cut the tubular structures.

The formation mechanism of the clastic dikes seems to be related to lateral spreading and hydraulic fracturing mechanisms (Obermeier, 1990). The orientation of the main system (145°) perpendicular to the slope and its greatest thickness and continuity in relation to the other systems could be explained by a mechanism of lateral spreading. Lateral spreading reflects translational movement downslope and separation between individual blocks where shaking has been especially strong (Obermeier et al., 1993). Movement occurs where there is only minor resistance to lateral translation of the cap sitting on liquefied sediment. Besides lateral spreading, the geometry of the dikes (145° and other directions), their orientation, injected material, apical terminations and central apertures all point to a hydraulic fracturing mechanism.

The sand formation also shows numerous tubular structures in the shape of vents with diameters of 8 to 20 cm, whose greatest density coincides with a zone close and parallel to the scarp that marks the surface evidence for fault F1 (Figure 3). These tubes have a very compact peripheral ring with secondary infilling materials of loose sand inside them. Owing to the greater compactness of the ring, erosion has preserved the structures and these may be seen in the outcrops. These structures are present from the lower layer H2 upwards and cross the upper layer H1 (Figure 7). In



Figure 6. General view of the seismite zone showing an abundance of tubular vents. For scale purposes the height of the paleoseismic features is between 20 and 30 cm.



Figure 7. Longitudinal section of a tubular vent affecting layers H1 and H2. For scale purposes the hammer is 30 cm long.

the zone of greatest density, 3 to 5 tubes occur per  $m^2$ ; the average being around 2 tubes per  $m^2$ .

#### Origin of the liquefaction features

To establish the origin of the liquefaction structures, possible causes of both seismic and aseismic nature were analyzed. The following causes were considered:

**Volcanic activity.** This can generate structures that give rise to vents or tubular conduits, injection of materials, fractures, infills, alterations, etc., as a consequence of the ejection of fluids, gases and materials. The last volcanic episode registered in the area took place over 100,000 years ago, while the age of the beach deposits is of the order of 10,000 years. The dikes and vents only affect the paleobeach deposit and not the tuffs of the substrate, ruling out a possible direct volcanic origin, although hydrothermal processes are being investigated, as a potential secondary process related to the tubular vents.

**Biological origin.** Some marine and coastal organisms can produce channels and orifices in beach deposits. However, the size, geometry and arrangement of the structures analyzed preclude this possibility (Calvo, pers. comm., 2002).

**Pressure waves and tsunamis.** Tsunamis produced by large offshore displacements of the sea bottom



*Figure 8.* Clastic dikes in the area of greatest density of liquefaction features. For scale purposes the dikes' height is between 5 and 10 cm, and their length is tens of meters.



*Figure 9.* Clastic dikes showing a central aperture and large vent. For scale purposes the hammer's length is 30 cm.

are highly improbable in this zone. The most recent landslide, in the valley of Guimar (35 km east of El Medano), occurred around 0.8 Ma (Masson and Watts, 1995). Although tsunamis or submarine slope failures of seismic origin cannot be ruled out, deposits associated with these have not been found in the study area. Nevertheless, this hypothesis is unlikely given

the distribution and orientation of the liquefaction structures.

Artesian pressures. The morphological and hydrogeological conditions of the zone exclude this possibility.

The evidence supporting a seismic origin includes: Upward directed hydraulic forces would be exerted

rapidly or almost instantly. The formation of dikes with the injection of sands transported from a source area by high-energy upward directed hydraulic forces, the apertures or double rims in the dikes and their apical terminations indicate mechanisms of hydraulic fracturing at high pressures. The geological evidence shows that virtually all the dikes must have a seismic liquefaction origin, and could almost certainly have formed solely in response to hydraulic fracturing (Obermeier, 1996). The direction of the tabular dikes is not random as would be expected if the dikes had originated by non-seismic mechanisms. The granulometric characteristics of the sand layers and their high uniformity, geological age and origin, geomorphological conditions and depth of the water table (discussed below), along with the resistance of the sands in which the structures developed are indicative of a high susceptibility of the deposits to liquefaction.

On the basis of the above evidence we can rule out a possible non-seismic origin and propose a seismic origin. This idea is also consistent with the seismotectonic characteristics of the region and the proximity of the previously described faults. The principal mechanism giving rise to the structures analyzed, also known as seismites, was liquefaction of the lower layer H2 that was composed of saturated sands. Due to the effect of intense interstitial pressures, water and sand were transported and expelled towards the surface via the vents, forming sand blows or craters by sand explosion. Hydraulic fracturing or lateral spreading led to rupture of the upper layer H1 of compact sands, giving rise to sand dike injection. The possibility of more than one earthquake occurring in the zone should not be precluded because of the presence of dikes cutting the vents, possibly implying more than one phase of liquefaction.

The beach sands formation has been dated by thermoluminescence as Holocene (Millán et al., 2002 as  $10,081 \pm 933$  years BP). The calcareous crusts that cover some of the liquefaction structures have been dated by the same technique at  $3490 \pm 473$  years BP. According to these data, liquefaction and the seismic phenomenon that produced it took place prior to 3490 years ago but after 10 ka.

### **Estimates of acceleration and magnitude of the paleoearthquake**

The force of a seismic event and the magnitude of a paleoearthquake can be estimated by several methods.

These have been reviewed in detail by Obermeier et al. (2001). The following methods are applicable to the present case:

- (a) The cyclic stress method based on estimates of the lower-bound peak ground acceleration at individual sites of liquefaction.
- (b) The Isihara method, which uses dike height at the site of hydraulic fracturing to estimate the actual value of peak ground acceleration at the site.
- (c) The magnitude bound method, which uses the furthest distance from the seismic source to the liquefaction zone.
- (d) Energy based solutions.

Methods (a) and (b) serve to calculate the peak acceleration needed for liquefaction to start at a particular site. The cyclic stress method is based on the method of Seed and Idriss (1971) and subsequent updates by Seed et al. (1985) and Youd and Noble (1997). Its application requires the interpretation of the soil profile at the time of liquefaction. To this end, we took into account the current conditions of the sand deposit and the aging processes to which the soil has been subjected from the time of liquefaction to the present.

The most common aging processes are (Olson et al., 2001): destruction of pre-earthquake soil structure and aging effects during liquefaction; post-liquefaction consolidation and densification, and post-liquefaction aging. The main outcome of liquefaction is increased granular packing, which may compact the sediment by some 27% (Owen, 1987). Following deposition, natural and man-made deposits develop a structure resulting from post-depositional mechanical readjustment and possible weak chemical bonding at particle contacts. This process is referred to as aging. The development of soil structure results in the improvement of soil properties such as shear strength, modulus, and penetration resistance (Schemertmann, 1991).

The present uplifted sand beach deposits show evidence of these aging processes. The main factors that have contributed to the compaction and partial cementation of the upper H1 layer are the uplift of the deposits by tectonics and the resultant downdropping of the water table, the geochemical conditions of the environment that favored an input of calcium carbonates and aluminum silicate compounds, and the extremely arid climatic conditions. Sands that could reflect conditions predating the aging processes were identified. These sands occur in the vicinity of the site closest to the coast and show the typical site granulometry and composition. Prior to liquefaction, the soil profile may have been as follows:

- An upper layer H1 formed of coarse to medium sands, dense to very dense with less than 2% fines, apparent natural density  $1.7 \text{ g/cm}^3$  and  $N_{\text{SPT}}$  (number of blows of the standard penetration test or SPT, ASTM – D1586) equal to or more than 30 blows. Estimated mean layer thickness was 2 m. The water table would have lain towards the base of this layer, and would have been subjected to variations in the water table. Its behavior could correspond to that of a hard, semi-confining and nonliquefiable layer.
- A lower layer H2, comprising medium to coarse sands, relative density intermediate, containing less than 2% highly uniform fines, apparent natural density  $1.5 \text{ g/cm}^3$  and  $N_{\text{SPT}}$  between 15 to 20 blows. The water table would lie above this layer and it would therefore be saturated. Mean estimated layer thickness is 1 m. This layer would have acted as a source zone for liquefaction.
- Layer T1 containing red tuffs weathered to 0.5 m thick paleosols.
- Layer T2, substrate composed of massive, very compact tuffs.

The cyclic stress method was applied following these hypotheses to estimate the peak ground acceleration (pga) necessary for the soil to undergo liquefaction. The results obtained give an acceleration of 0.22 g for  $(N_1)_{60} = 15$  and 0.30 g for  $(N_1)_{60} = 20$ . According to Youd and Noble (1997), this would correspond to a 50% probability of liquefaction.

The Ishihara (1985) method considers that the maximum height of liquefaction dikes is controlled by two factors: the thickness of the liquefied sediment and the pga. This method is valid for seismic structures produced by hydraulic fracturing. It is applicable where the cap thickness is reasonably uniform and when source sands range from very loose to moderately compact, at least for earthquakes of moment magnitude  $M \sim 7.5$  or larger, (Obermeier, 1998). It was considered that the hard, semi-confining, non-liquefiable layer was 2 m in thickness and a thickness of 1 m was assumed for the liquefiable source. For these conditions, the resulting pga was 0.35 g according to the Ishihara method. Bearing in mind that the cyclic stress method represents the minimum acceleration value, and Ishihara method considers average conditions, a representative value of 0.30 g was selected from the possible range between 0.22 and 0.35 g.

From the accelerations calculated, intensities at the site can be estimated using one of the avail-

able empirical expressions. The equation used in the Spanish Seismic Code is:  $I = [3.2233 + \log_{10}(a/g)]/0.30103$ , where  $I$  are intensities,  $a$  is the horizontal pga ( $\text{cm/s}^2$ ) and  $g$  is in % gravity. Hence an acceleration of 0.30 g gives a predicted intensity of IX.

The magnitude of paleoearthquakes, in terms of the moment magnitude  $M$ , can be calculated using the magnitude bound method and energy based approaches. The magnitude bound method estimates the magnitude of a paleoearthquake using relations between earthquake magnitude and the distance from the tectonic source to the farthest site of liquefaction. It is based on worldwide historical earthquakes (Ambraseys, 1988) and the data described by Obermeier et al. (1993) and Pond (1996). This method requires the identification of the seismic source. In the present case, the closest seismic sources are found between Tenerife and Gran Canaria over a line of epicenters in the ocean, at an approximate distance of 35 km from the El Médano site (Figure 2C). This source is associated with a NE–SW trending fault that runs parallel to the eastern coast of Tenerife, and was inferred from gravimetric data by Bossard and McFarlane (1970). In 1989, this fault produced the greatest earthquake instrumentally recorded on the archipelago ( $M = 5.2$ ). The length attributed to this fault is 30 km (Mezcua et al., 1992), yet it extends to over 80 km. A further possible seismic source is fault F1 located at the site. Its prolongation beneath the ocean was established by reflection seismic profiles indicating a minimum length of 5 km. However, the instrument record makes no reference to earthquakes with epicenters close to this fault, so that we only consider the submarine fault 35 km from the site as a seismic source when calculating the earthquake's magnitude, which yielded a magnitude  $M$  in the range 6.4 to 6.8. Given that 6.4 is the lower limit of the data considered by Ambraseys (1988), we took a  $M = 6.8$  as being representative. Wells and Coppersmith's (1994) relationship between fault length and magnitude also gives a  $M = 6.8$ .

The second method used to estimate magnitude is based on so-called energy-based approaches that relate magnitude to energy release (Davis and Berrill, 1982) and subsequent reviews by Berrill and Davis (1985) and Trufinac (1995). This method relates magnitude to distance from the epicenter, to the liquefaction site and the  $(N_1)_{60}$  (number of blows of the SPT for a pressure of  $10 \text{ t/m}^2$  and an effective energy of 60%). For  $(N_1)_{60} = 20$ , the results obtained indicate a magnitude  $M = 6.8$  according to the method of Berrill and

Davis (1985) and of 7.2 according to that of Trufinac (1995).

In summary, the magnitudes estimated are in the range 6.4 to 7.2; a value of  $M = 6.8$  being considered the most representative. These estimates were based on the assumption that the seismic source was the submarine fault. If fault F1 as being closer to the site was the source of seismicity then models predict lower magnitudes but similar accelerations.

## Conclusions

Several liquefaction structures were identified in El Médano, in southern Tenerife. These structures were clastic dikes and tubular vents; their origin being attributed to the liquefaction of sands by an earthquake of great intensity.

The mechanisms that gave rise to the clastic dikes were hydraulic fracturing and lateral spreading of a layer of compact sands in response to high pore pressures of seismic origin. These pressures, in turn, led to the movement and injection of sands across the compact sands level. The vents are the result of high upward hydraulic pressures causing the ejection of water and sand through these conduits to the surface, possibly forming sand blows and explosion craters.

The peak ground acceleration needed to produce liquefaction and the sand dikes was estimated at 0.22 to 0.35 g. An acceleration of 0.30 g, considered to be the most characteristic, would correspond to an intensity of IX at the site of liquefaction. The magnitude of the earthquake causing liquefaction was calculated to be in the range 6.4 to 7.2 with a value of  $M = 6.8$  taken to be representative. This result was obtained assuming that a submarine fault was the seismic source.

The liquefaction structures developed over a tectonically uplifted beach of sand deposits dated as  $10,081 \pm 933$  years BP. Over these sands and liquefaction structures, fine calcareous crust levels dated as  $3490 \pm 473$  years BP were observed. The paleoearthquake responsible for liquefaction occurred during the Holocene; its age lying between these two dates. Nevertheless, tectonic and geomorphological data from field observations suggest an age closer to the younger constraint.

Two faults F1 and F2 aligned in a direction  $N55^\circ$  close to the liquefaction site were identified. Fault F1 cuts the uplifted beach sand formation. Through seismic reflection profiles, its extension under the sea was

identified, and a minimum length of 5 km was established. Both faults limit a small graben, which gives rise to a depression in whose approximate center there are several lagoons.

Possible seismic sources near the site of liquefaction were considered. The main source is inferred to have been a submarine NNE–SSW trending fault some 35 km from the site between the islands of Tenerife and Gran Canaria. Its movement takes the form of a sinistral thrust. This fault shows associated seismicity. Another proposed source is fault F1, which affects the sand formation where the paleoliquefaction is found. No historical epicenters related to this fault have been recorded.

The tectonic structures affecting materials of recent age and the seismicity associated with these structures demonstrates existing seismotectonic relationships and confirms the paleoseismic activity identified in southern Tenerife. The paleoearthquake investigated here is the largest of those registered on the Canary Islands.

The presence of active faults affecting materials of very recent age and their association with a paleoearthquake of high intensity in the south of Tenerife are key factors that need to be borne in mind when evaluating seismic hazards on the Canaries, a region, which up until now, had been considered to be of low seismic activity.

## Acknowledgements

We are grateful to Dr. A. Millán of the Universidad Autónoma de Madrid for carrying out the thermoluminescence procedures. Dr. S. Obermeier from the US Geological Survey (Emeritus), Professor F. Ricci Lucchi of the Università di Bologna and Professor J. P. Calvo of the University Complutense of Madrid are thanked for their helpful comments and advice. Thanks are also due to Dr. M. A. Rodríguez Pascua and P. Llanes for providing useful information. Finally, we are grateful for the efforts of reviewers whose comments have helped improved the manuscript.

## References

- Ambraseys, N. N. 1988. Engineering seismology. *Earthq. Eng. Struct., D.*, **17**(1), 1–105.
- Berril, J. B. and Davis, R. O. 1985. Energy dissipation and seismic liquefaction of sands revised model. *Soils and Found.*, **25**(2), 106–118.

- Bosshard, E. and MacFarlane, D. J. 1970. Crustal structure of the western Canary Islands from seismic refraction and gravity data *J. Geophys. Res.*, **75**, 4901–4918.
- Davis, R. O. and Berril, J. B. 1982 Energy dissipation and seismic liquefaction of sands. *Earthq. Eng. Struct. D.*, **10**, 59–68.
- Dziewonski, A. M., Ekström, G., Woodhouse, J. H. and Zwart, G., 1990, Centroid-moment tensor solutions for April–June 1989, *Phys. Earth Planet. Int.* **60**, 243–253.
- Ishihara, K. 1985. Stability of material deposit during earthquakes. *Proc. 11 th. Int. Conf. Soil. Mech. and Found. Eng.* San Francisco, Vol I. 321–376. A. A. Balkema, Rotterdam.
- Llanes, P., Muñoz, A. Muñoz-Martín, A., Acosta, J., Herranz, P., Carbó, A., and Palomo, D. Morfological and structural analysis in the Anaga offshore massif, Canary Islands: fractures and debris avalanches relationships. *Mar. Geophys. Res.*, (in this volume).
- Mezcua, J., Burforn, E., Udías, A. and Rueda, J., 1992. Seismotectonic of the Canary Islands. *Tectonophysics*, **208**, 447–452.
- Millan, A., Benitez, P. and Calderón, T. 2002. Datación absoluta por termoluminiscencia de muestras de paleoplayas de Tenerife. Lab. Datación y Radioquímica. Universidad Autónoma de Madrid. España. (Unpublish).
- Obermeier, S. F. 1996. Use of liquefaction -induced features for paleoseismic analysis. *Eng. Geol.*, **44**, 1–76.
- Obermeier, S. F. 1998. Overview of liquefaction evidence for strong earthquakes of Holocene and latest Pleistocene ages in the states of Indiana and Illinois, USA. *Eng. Geol.*, **50**, 227–254.
- Obermeier, S. F., Martin, J. R., Frankel, T. L., Munson, P. J., Munson, C. A. and Pond, E. C. 1993. *Liquefaction evidence for one or more strong Holocene earthquakes in the Wabash Valley of southern Indiana and Illinois.* U.S. Geol. Survey Prof. Paper, **1536**, 27 pp.
- Obermeier, S. F., Pond, E. C. and Olson, S. C. 2001. *Paleoliquefaction studies in continental settings: geological and geotechnical features in interpretations and back-analysis.* U.S. Geol. Survey. *Openfile Report*, **01–29**. 75 pp.
- Olson, S. M., Obermeier, S. F. and Stark, T. D. 2001. Interpretation of penetration resistance for back analysis at sites of previous liquefaction. *Seism. Res. Lett.*, **72**(1), 46–59.
- Owen, H. G. 1987. *Deformation processes in unconsolidated sands.* In: *Deformation of Sediments and Sedimentary Rocks.* Jones, E. M. and Preston, M. F. (Ed.), Geol. Soc. of London, Publ. **29**, 11–24.
- Pond, E. C. 1996. *Seismic parameters for the central United States based on paleoliquefaction evidence in the Wabash Valley.* Ph.D. Thesis. Virginia Polytech. Inst. Blacksburg, Virginia, 583 pp.
- Schemertmann, J. H. 1991. The mechanical aging of soils. *J. Geotech. Eng-ASCE*, **117**(1), 1288–1330.
- Seed, H. B. and Idriss, I. M. 1971. Simplified procedure for evaluating soil liquefaction potential. *J. Soil Mech. Found. Div. ASCE*, **97**(1), 1249–1273.
- Seed, H. B., Tokimatsu, K., Harder, L. F. and Chung, R. M. 1985. Influence of SPT procedures in soil liquefaction resistance evaluations. *J. Soil Mech. Found. Div. ASCE*, **111**, 1425–1445.
- Trifunac, M. D. 1995. Empirical criteria for liquefaction in sands via standard penetration test and seismic wave energy. *Soil Dyn. Earthq. Eng.*, **14**, 419–426.
- Wells, D. L. and Coppersmith, K. J. 1994. New empirical relationships among magnitude, rupture length, rupture area, and surface displacement. *B. Seismol. Soc. Am.*, **84**, 974–1002.
- Youd, T. L. and Noble, K. 1997. Liquefaction criteria based on statistical and probabilistic analysis. *Proc. NCEER Workshop on Evaluation of Liquefaction Resistance of Soils.* Youd, T. L. and Idriss, I. M. (Eds.), Tech. Rep. NCEER-97-0022, State University of New York at Buffalo, New York, 210–216.